Materials Science

Trade Science Inc.

An Indian Journal

Full Paper

Microwave-assisted preparation of Cu$_x$S/ polymer nanocomposite: Effects of the annealing temperature on the structural and the optical properties

Lotfi Orimi Rahim[1], Bour Meysam[2], Asghari Jila*[3], Lashkarbolouki MohammadReza[1]
[1]Department of Physics, University of Golestan, Gorgan, (IRAN)
[2]Department of Physics, Islamic Azad University of Qum, (IRAN)
[3]Department of Chemistry, University of Golestan, Gorgan, (IRAN)
E-mail: asghari_jila@yahoo.com

ABSTRACT

Synthesis of Cu$_x$S (1<x=2) nanocomposite on the surface of polyacrylamide (PAM) was evaluated by chemical reaction of sulfur powder, cupper nitrate and acrylamid in ethylene glycol as solvent by using microwave irradiation. We have shown that the annealing temperatures of Cu$_x$S nanocomposite powder under Argon atmosphere in the various temperatures; 100 °C, 200°C, 300 °C and 400 °C are more important in the ratio of Cu$_x$S to CuS. The synthesized particles were then characterized by powder x-ray diffraction, and then the crystalline structure of the Cu$_x$S nanocomposite has been transformed from rhombohedral to hexagonal structure by increasing the temperature. UV-Vis and photoluminescence spectrum have shown a red shift (2~5 nm) when increases the annealing temperature.
© 2012 Trade Science Inc. - INDIA

KEYWORDS

INTRODUCTION

Copper sulfides (Cu$_x$S 1=x=2) are interesting materials due to their special physical and chemical properties. The properties of Cu$_x$S are affected by the accurate stoicheiometry, this is depending on the conditions of preparation. There are several stable phases of copper sulfides at room temperature with a wide variety of compositions (x=2, 1.95, 1.8, 1.75, 1)[1-5]. Cuprous sulfide (Cu$_2$S) is considered as an ideal absorber in the photovoltaic conversions[6]. Cu$_2$S is well known to be a p- type semiconductor with shallow Cu vacancy acceptors. It has a direct band gap of 1.2 ev and

an indirect band gap of 1.8 ev and an electron affinity of 4.3 (ev). Cu$_2$S among p-type semiconductor including SnS and Ag$_2$S, is a good candidate for the heterojunction solar cells due to the band gap and a simple fabrication method[7-9].

Cu$_2$S has been developed rapidly in semiconductor industries because of its unique optical properties and potentially high absorption coefficients[10]. Cu$_x$S is used as a carrier charge in solar cells because of its optical properties and it has useful applications in a wide range of areas such as solar control coatings, solar energy conversion, electronic and low-temperature gas sensor[11-16].

If this nanocomposite is used in optoelectronic de-

Full Paper

vices, the optical and electrical efficiency of the pro-posed device will highly depend on the annealing tem-perature. Meanwhile, the annealing temperature not only has an effective role in achieving a stable crystalline struc-ture combination, but it causes a shift of the signal emis-sion and absorption of sample.

One of the important issues in preparation various nanostructures of Cu_xS, is the existence of different sto-ichiometry of Cu in the composite (where x the range of 1=x=2 can be changed). It is mainly because of ca-pability of CuS in achieving practical efficiencies[17]. Change in the crystalline structure with increasing the coefficient copper components and conversion of Cu_xS to CuO due to the annealing is one of the challenges in preparing this kind of material. Physicist and chemist are very interested in achieving the optimum combina-tion of x in Cu_xS, and preparation of nanomaterials with optical and structural properties which is considered to be favorable for many industrial processes. Different processes are used to produce Cu_xS. These methods are focused on nanowires[18], nanocomposite in poly-mer template[19], nanorods, nanolayer[20], spherical nanoparticles[21-22] and quantum dots[23]. Many authors have studied the structural and optical properties of chemically deposited Cu_xS thin films[24-32].

Polymer with thin sulfide layers belongs to the com-posites. Such composite materials are of particular in-terest for the fabrication of substrates for deposition of metal and semiconductor, solar selective coating, solar cells, photoconductor, sensor, etc.[33, 34]. Practical ap-plication of copper sulfide coatings in the various fields of engineering stimulates interest toward developing a new technology.

In this article, we will describe preparations of nanocomposite Cu_xS along with an investigation of the effect of annealing temperature on the distribution of copper and sulfur. Characterization of their structural and optical properties is investigated using X-ray dif-fraction (XRD), Transmission electron micrograph (TEM), UV-Vis spectrum and photoluminescence (PL) emission.

MATERIALS AND METHODS

Materials

Sulfur powder, copper nitrate, acryl amide, ethyl-

ene glycol, etc. were purchased from Aldrich chemical company and have been used as we received without further purification. Double- distilled water equipment is used for this experiment.

Characterization

Optical absorption spectra of nano-Cu_xS in poly-mer films are recorded with a Shimatzo-1600 Ultra-violet/ Visible (UV-Vis) spectrometer over a range of wavelength from 200 to 900 nm. X-ray diffraction (XRD) measurements are performed on a Bruker D8 ADVANCE diffractometer and the patterns were re-corded using CuKa irradiation (λ= 1.54178 °A). Pho-toluminescence spectrum (PL) of modified Cu_xS col-loidal solution was achieved on an Elemer LS-80 fluo-rescence spectrophotometer using a 200-900 nm ex-citation line. Transmission electron microscopy (TEM) was undertaken on a Zeiss EM10C instrument. Micro-wave-assisted reaction was performed using a micro-wave cavity (2.45 GHz, maximum power 1000w, Mileston) equipped with a condenser, and the reaction temperature 190 °C was controlled via the fiber-optic sensor.

Preparation of nano Cu_xS/ polymer composites

Acrylamide (AM) (2.132 gr, 0.03 mole) is dis-solved with an appropriate ratio of ethylene glycol (300 cc) in a round bottom schlenk flask. Then, solid cupper nitrate (7.24 gr, 0.0386 mole) and sulfur powder (0.96 gr, 3.75 mmole) are added slowly under magnetic stir-ring at the room temperature. The mixture was stirred at the room temperature for 10 minutes. The suspen-sion was maintained into a microwave oven equipped with a condenser under power 400 W at 190 °C for 30 minutes. Subsequently, the dark brown solid products were being centrifugalized which is followed by three fold washing with ethanol and de-ionized water. After re-centrifugalizing, the products were finally dried at 75 °C in an electrical oven for half an hour. Dried powder nanoparticles were annealing at the temperatures 100, 200, 300 and 400 °C, respectively in two different Ar-gon and Air atmospheres. Nanoparticles of Cu_xS have been characterized using X-ray diffraction (XRD), trans-mission electron microscopy (TEM), UV-Vis and pho-toluminescence spectrum (PL) which are based on the optical, structural and thermal characterization.

RESULTS AND DISCUSSION

X-ray diffraction analysis

The crystalline nature of Cu_xS particles and the identification of elements and the analysis of their structures in the resulting compound were characterized by the XRD spectra. The crystallographic planes of XRD spectra (Figure 1) were indexed using Bragg's law for the x-ray diffraction and are compared with those of Row data software with reference codes of CuS (hcp), Cu_2S (cubic) and Cu_xS respectively[35]. The XRD patterns of these nanoparticles reveal the two crystalline structures Cu_xS (1<x<2) and CuS perfectly. The ratio of the products, that is Cu_xS-CuS, the crystallinity and then the yield of it strongly depend on the reaction of the annealing temperature. With increasing the annealing temperature in the air atmosphere the ratio of Cu_xS to CuS is increased.

The annealing temperature in two different atmospheres and intensities of MW irradiation are the main factors that control the final output of the reaction, (Figure 1 and 2). Hence, the phase composition of Cu_xS nanocomposite varies with increasing the value of x as we found in our investigation. Moreover, with increasing the stoichiometry of x, the shape of crystalline structure was changed from rohomhedral to hexagonal.

We found that the required time and power for turning of transparent solution into golden brownish is reduced at the higher temperature (160 °C) and power (400 w). It is because of the fact that the formation rate of free ions at a fixed ion concentration depends on the deposition temperature. If the composition temperature is high, then the free ions deposit on the AM surface along with interaction with each other within the solution and hence, the color of the solution changes rapidly. For deposition of copper and sulfur on the films, the availability of nucleation centers over the substrate is necessary. Such centers are normally formed through the formation of metal ions complexes over the acrylamide and ethylene glycol which would thereby form an initial layer of the metal ciliate. This initial layer acts as a catalytic surface and this surface is crucial for a uniform deposition of thin films on the surface. The deposition of the thin film takes place through the condensation of the copper and the sulfide ions which are readily provided in the MW oven.

As discussed above, the substrate temperature has more influence on the composition and the morphology of the powder. It was determined that a value of x in the Cu_xS layers varies within the internal 1<x<2, so that produced composition was a mixture of covellite Cu_xS. By studding of Cu_xS layers using X-ray diffraction, we detected three phases: with x= (1.7-1.96) the phase composition of Cu_xS depends on the annealing temperatures in air and Ar atmosphere. The XRD spectra recorded for the Cu_xS thin film before and after increasing the annealing temperature were shown, (Figure 1).

Generally, the annealing temperatures at (100-300 °C) in argon atmosphere favors the obtained of copper-rich phase (Cu_xS, x= 1.7-1.96). According to our results to achieve the nanomaterial composition Cu_xS with x>1.7 in Ar atmosphere the optimum annealing temperature is 300 °C. With air atmosphere and the temperature higher than 400 °C we found $CuSO_4$ and with increasing the temperature up to 5oo°C CuO was produced, respectively. Meanwhile the grain size of copper sulfide with increasing the annealing temperature is increased (Figure 1 and 2). The average size of the annealed film at a higher absorption is 30 nm. During annealing the sample at 400 °C the particle size of the sample was grown on the acrylamide substrate with an average diameter of 100 nm which reveals amorphous nature of the materials. The grain size of copper sulphide is calculated using the Scherer's relation:

$$t = \frac{k\lambda}{\beta \cos \theta}$$

Where β is the broadening of the diffraction line measured at the half maximum intensity (radian) and the wavelength of the Cu kα X-ray, i.e. λ= 1.54056 A°. The average grain size was determined to be averaged 30 nm. With increasing the annealing temperature to 400 °C, the particle size of Cu_xS composition was grown with an average diameter of 100 nm. Furthermore, the annealing temperature increased the efficiency of Cu_xS peaks and deleted or decreased the intensity of the peaks of impurity. For example, when annealing temperature of Cu_xS is increased to 300 °C, the intensity of the peaks at 2θ= 30, 39, 59 °C completely vanishes as far as relates to impurity. On the other hand, crystalline layer of Cu_xS grows with increasing the an-
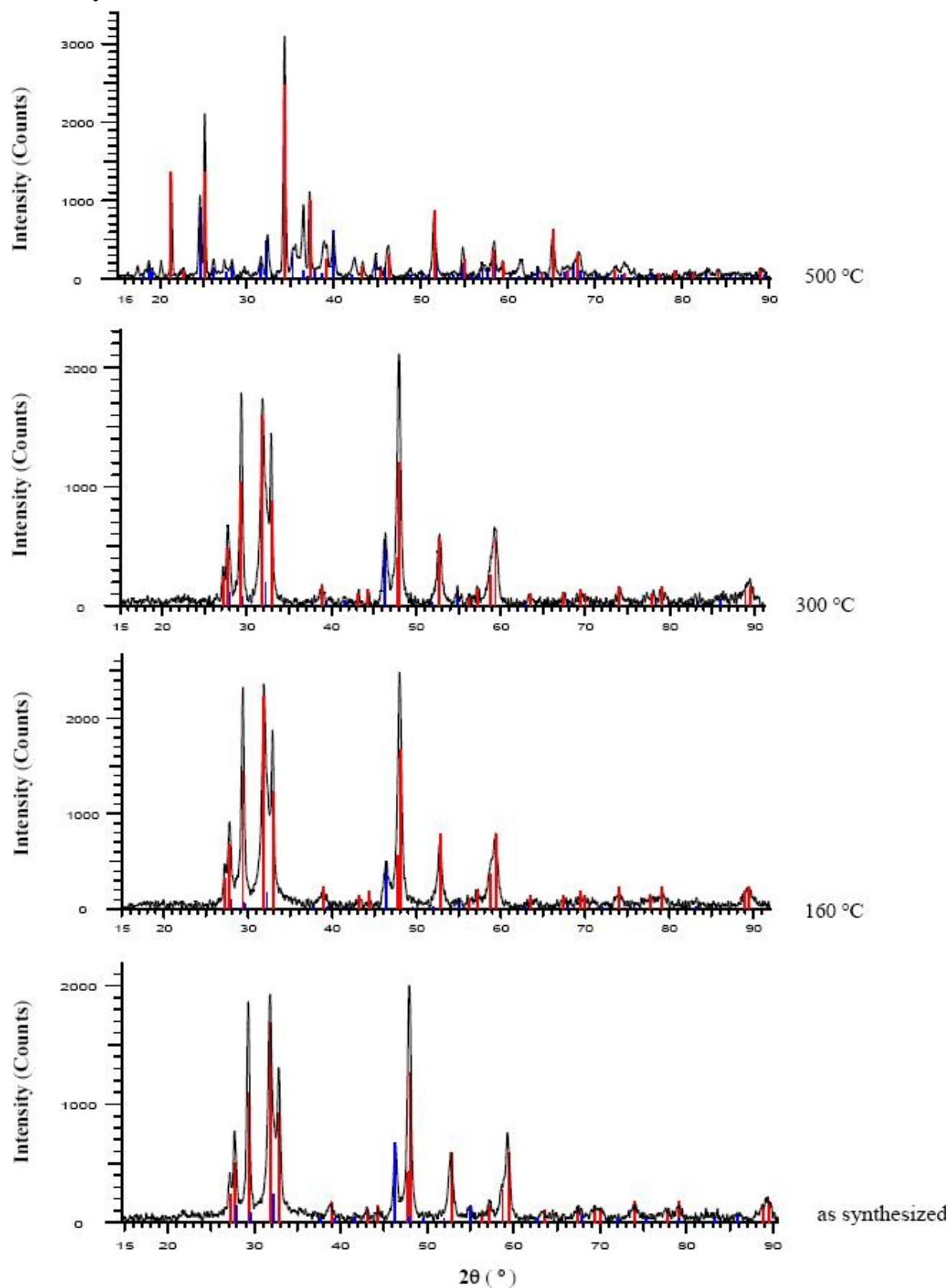
Full Paper

Figure 1 : XRD spectrum of (a) Cu_xS thin film, (b) as-prepared Cu_xS film deposited with different annealing temperatures in air atmosphere
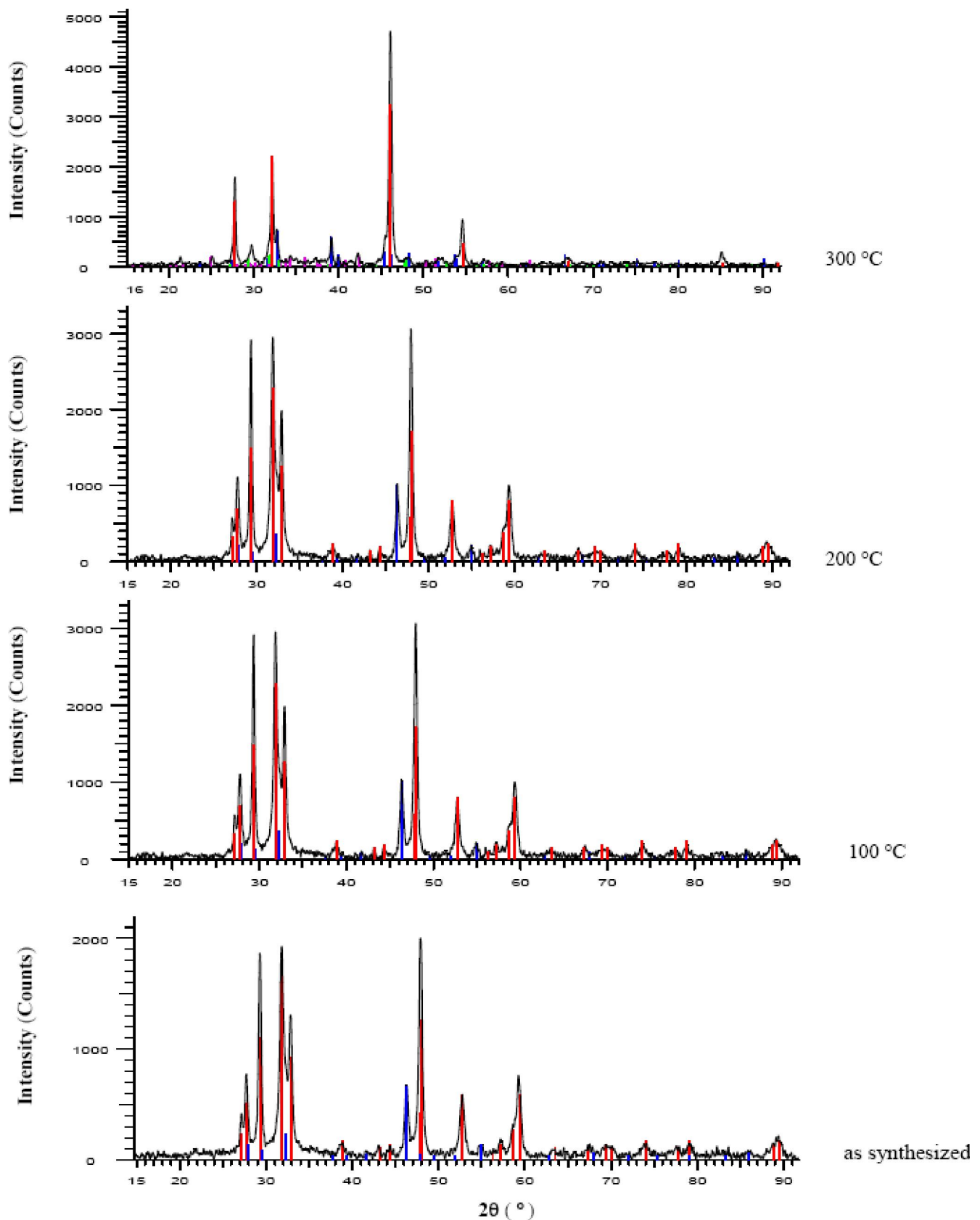
Figure 2 : XRD spectrum of (a) Cu$_x$S nanoparticle, (b) as-prepared Cu$_x$S nanoparticle deposited with different annealing temperatures in argon atmosphere
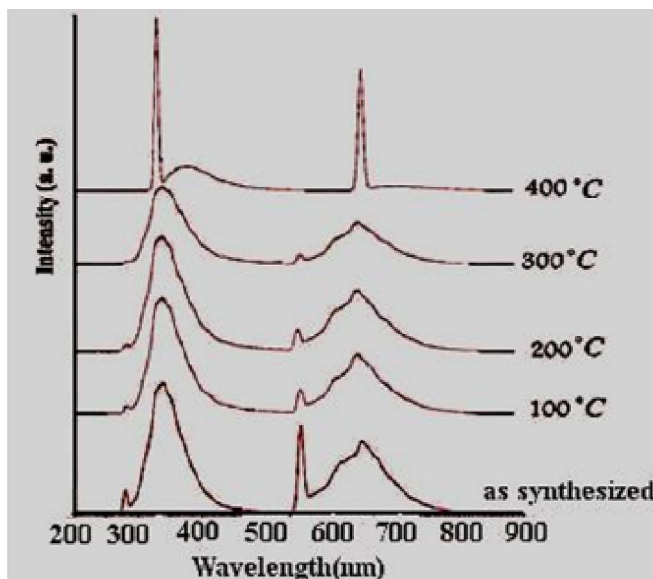
Full Paper

Figure 3 : PL spectra of synthesized and annulated sample
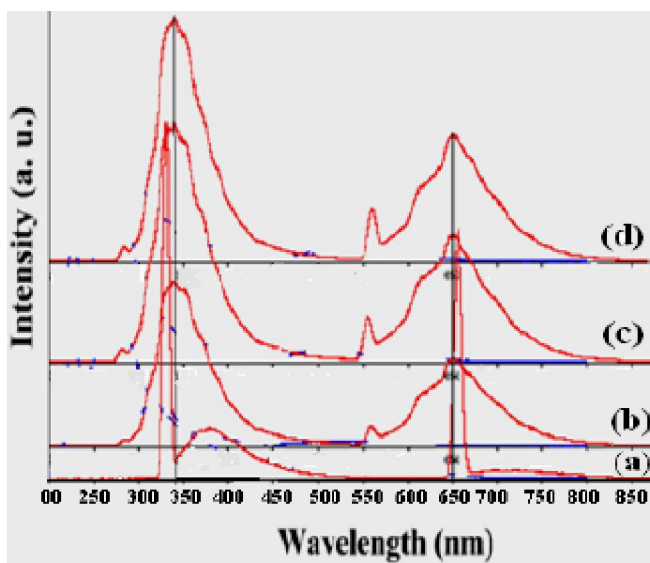

Figure 4 : PL spectra of real solution and residual solution after: a) one time b) two time c) three time washing

nealing temperature and it has high diffraction intensity in comparison to the synthesized sample (without annealing). We found it in the diffraction patterns 102.

Photoluminescence (PL) analysis

The PL spectra of powder Cu_xS and its annulated compounds from it were determined at different temperatures using the excitation wavelength 275 nm. The distinct PL emissions have been detected at 342 nm and 662 nm, which are close to the reports for the excitation of S and Cu, respectively. The PL spectra of the residual solution after separation of the resulting powder and its dissolution are shown at the different stages,

(Figures 3 and 4). Comparison of PL spectra of the residual solution after making deposits in various stages of washing indicates an increment in the relative intensity of peaks, which is related to the impurities. This suggests, washing with ethanol is effective in the separation of impurities at each step. Emission spectra of the annulated samples at the different temperatures showed two major sharp peaks at the visible and the ultraviolet wavelengths for all samples, respectively. Comparison of the two spectra was indicated as a red shift transfers about 2 to 5 nm. We determined that the intensities of the resulted peaks are influenced by several parameters such as shape, size, impurity and crystallinity which are controlled by the temperature. With increasing the annealing temperature of sample, the intensities of signal is increased too, and the peak width is reduced. The enhanced efficiency of the obtained sharp peaks was due to the absence of impurity in the samples. In addition, the reduction of the peak width at the higher temperature is because of the uniform distribution of particles or deletion of the impurity in compounds. The first peak at PL emission is attributed to the transfer balances of surface near to the conductive band primarily related to the exited band of sulfur. But the second peak is attributed to the inter band electronic transition of Cu.

UV-Vis spectroscopy

Absorbance spectra of synthesized and annulated samples were shown in Figure 5. Calculation of particle size was carried out by Kayanuma equation[35]. Comparison of the absorbance wavelength edge of synthesized and annulated samples was revealed a red shift in the wavelength edge with increasing the annulated temperature. Absorbance wavelength edge in the absorbance spectra was exactly comparable to the first wavelength of the exited signal at the ultraviolet photo luminance region. The direct allowed optical band gap E_g can be expressed as a function (1) of the maximum wavelength using a relation:

$$E_g^{nano} (ev) = \frac{1240}{\lambda_{max} (nm)} \qquad (1)$$

Where $\lambda = 430$ and 560 nm are maximum wavelength edge, and the value of optical direct and indirect band gap (E_g) have been calculated as 2.21 and 2.88 ev respectively.

It was found that almost all the experimental data in a wide (10-35 nm) range of the Cu_xS nano composites size can be described by the effective masses approximation using the well known expression; Kayanuma:

$$\Delta E_g = E_g^{nano} - E_g^{bulk} = \frac{\hbar^2 \pi^2}{2MR^2} \qquad (2)$$

Where E_g^{bulk} is energy band gap of balk powder, E^{nano} is energy band gap of nanocrystalline Cu_xS, which is obtained from the wavelengh corresponding to the absorption edge of each specimen. Here, R is the particle radius, h is the reduced plank constant, and M is the effective mass of exitons in $\frac{1}{M} = \frac{1}{M_e} + \frac{1}{M_h}$ which M_e is effective mass of electron, M_h effective mass hole of electron and m_0 is the electron rest mass. Using these data in Eq. (2) we obtain the approximate particle size of the synthesized sample (without annealed) 30 nm. These are in agreement with the sizes determined from TEM and XRD.

In order to evaluate the effect of temperature on the size distribution of nanoparticle, we annealed the prepared sample at different temeratures. According to the absorption spectra We shown that with incresing the annealed temperature and band gap, the particle size of sample is incresed.
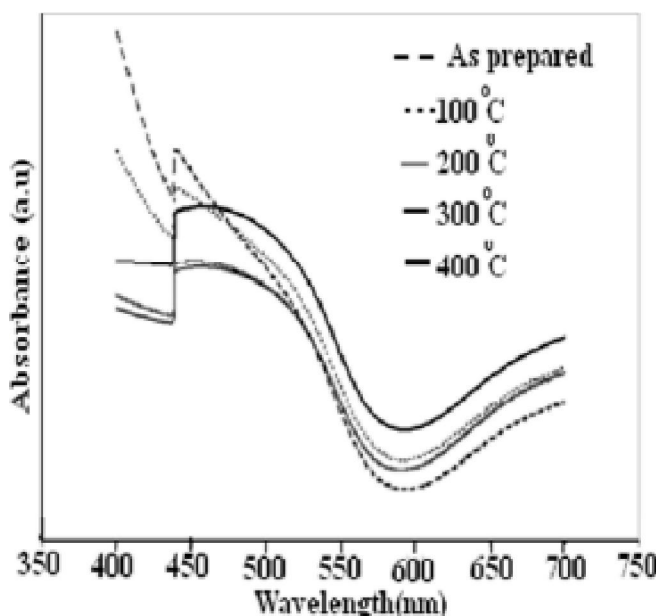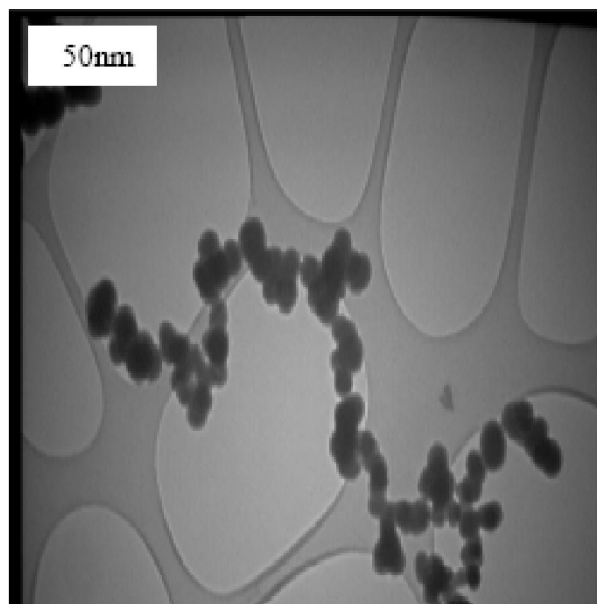

Figure 6 : Transmission electron micrographs of (TEM) of nanocomposite Cu_xS annealed 10 min at 400ºC

Transmission electron microscopy (TEM) analysis

Figure 6 displays a TEM micrograph of nano composite samples Cu_xS annealed at 400 ºC. It was indicated particle size of composite about 10-35 nm.

ACKNOWLEDGMENTS

REFERENCES

[1] I.Grozdanov, M.Najdoski; J.Solid State Chem., **114**, 469-475 **(1995)**.
[2] H.Grijavla, M.Inoue, S.Boggavarapu, P.Calvert; J.Mater.Chem., **6**, 1157-1160 **(1996)**.
[3] B.J.Mulder; Phys.Stat.Sol.A., **13**, 79-88 **(1972)**.
[4] Y.Xie, P.Yan, Y.T.Qiun; Chem.Lett., **7**, 655-656 **(1999)**.
[5] S.Kashida, K.Yamamoto; J.Phys.Condens.Matter., **3**, 6559-6570 **(1991)**.
[6] T.J.Coutts, J.D.Meakin; Current Topics in Photovoltaics, Academic Press, Florida, **(1985)**.
[7] A.P.Alivisatos; Science, **271**, 933-937 **(1996)**.
[8] C.B.Murray, C.R.Kagan, M.G.Bawandi; Science, **270**, 1335-1338 **(1995)**.

Figure 5 : UV-Vis absorbance spectra of synthesized and annealed sample at different temperature

Full Paper

[9] V.Kilmov, P.H.Bolivar, H.Kurz, V.Karavanskii, V.Krasovskii, Y.Korkishko; Appl.Phys.Lett., **67**, 653-655 **(1995)**.

[10] M.T.S.Nair, L.Guerrero, P.K.Nair; Semicound.Sci.Technol., **13**, 1164-1169 **(1998)**.

[11] J.Johansson, J.Kostamo, M.Karppinen, L.Niinisto; J.Matter.Chem., **12**, 1022-1026 **(2002)**.

[12] A.Setkus, A.Galdikas, A.Mironas, I.Simkiene, I.Ancutiene, V.Janickis, S.Kaciculis, G.Mattogno, G.M.Ingo; Thin Solid Films, **391**, 275-281 **(2001)**.

[13] A.Setkus, A.Galdikas, A.Mironas, V.Strazdiene, I.Simkiene, I.Ancutiene, V.Janickis, S.Kaciulis, G.Mattogno, G.M.Ingo; Sens.Actuators B.Chem., **78**, 208-215 **(2001)**.

[14] I.Grozdanov, M.Najdoski; J.Solid State Chem., **114**, 469-475 **(1995)**.

[15] W.Siripala, L.D.R.D.Perera, K.T.L.DeSilva, J.K.D.S.Jayanetti, I.M.Dharmadasa; Solar Energy Mater.Solar Cells, **44**, 251-260 **(1996)**.

[16] M.C.Breller, C.L.Torres Martinez, J.C.McNulty, R.K.Mehra, J.Z.Zhang; Pure Appl.Chem., **72(1-2)**, 101-117 **(2000)**.

[17] S.Wang, Q.Huang, X.Wen, X.Y.Li, S.Yang; Phys.Chem.Chem.Phys., **4**, 3425-3429 **(2002)**.

[18] J.F.Zhu, Y.J.Zhu, M.G.Ma, L.X.Yang, L.Gao; J.Phys.Chem., **C111**, 3920-3926 **(2007)**.

[19] L.Jiang, Y.J.Zhu; Mater.Lett., **63**, 1935-1938 **(2009)**.

[20] S.H.Park, Y.Xia; Adv.Mater., **10**, 1045-1048 **(1998)**.

[21] M.Yang, X.Yang, L.Huai, W.Liu; Appl.Surf.Sci., **255**, 1750-1753 **(2008)**.

[22] S.Li, H.Wang, W.Xu, H.Si, X.Tao, S.Lou, Z.Du, L.S.Li; J.Colloid Interface Sci., **330**, 483-487 **(2009)**.

[23] M.T.S.Nair, C.Lopez-Mata, Q.Gomezdaza, P.K.Nair; Semicond.Sci.Technol., **18**, 755-759 **(2003)**.

[24] J.Y.Gong, S.H.Yu, H.S.Qiann, L.B.Luo, X.M.Liu; Chem.Mater., **18**, 2012-2015 **(2006)**.

[25] G.W.Lather, S.M.Theberge, T.F.Rozan, D.Richard, C.C.Rowlands, A.Oldroyd; Environ.Sci.Technol., **36**, 394-402 **(2002)**.

[26] V.Klimov, P.H.Bolivar, H.Kurz, V.Karavanski, V.Krasovakii, Yu.Korkishko; Appl.Phys.Lett., **65**, 653-655 **(1995)**.

[27] K.M.Gadave, C.D.Lokhande; Thin Solid Films, **229**, 1-4 **(1993)**.

[28] C.A.Estrada, G.Alvarez, R.E.Cabanillas, P.K.Nair; J.Phys.D.Appl.Phys., **25**, 1142-1147 **(1992)**.

[29] A.A.Sagade, R.Sharma; Sensor Actuat. B.Chem., **133**, 135-143 **(2008)**.

[30] M.A.Zhukovskiy, A.L.Stroyuk, V.V.Shvalagin, N.P.Smirnova, O.S.Lytvyn, V.V.Shvalagin, N.P.Smirnova, O.S.Lytvyn, A.M.Eremenko; J.Photoch.Photobio.A., **203**, 137-144 **(2009)**.

[31] C.G.Munce, G.K.Parker, S.A.Holt, G.A.Hope; Physicochem.Eng.Aspects, **295**, 152-158 **(2007)**.

[32] R.S.Mane, C.D.Lokhande; Mater.Chem.Phys., **65**, 1-31 **(2000)**.

[33] A.Galdikas, A.Mironas, V.Strazdiene, A.Setkus, I.Ancutiene, V.Janickis; Sensor.Actuat.B-Chem., **67**, 78-83 **(2000)**.

[34] Powder Diffraction Files [5]. JCPDS- ICDD, USA, PA, 19073-3273, **(2001)**.

[35] Y.Kayanuma; Phys.Rev.B., **38**, 9797-9805 **(1988)**.